

Quadruply Bonded Dimetal Units Supported by 2,4,6-Triisopropylbenzoates $\text{MM}(\text{TiPB})_4$ ($\text{MM} = \text{Mo}_2$, MoW , and W_2): Preparation and Photophysical Properties

Brian G. Alberding,[†] Malcolm H. Chisholm,^{*,†} Yi-Hsuan Chou,[‡] Judith C. Gallucci,[†] Yagnaseni Ghosh,[†] Terry L. Gustafson,^{*,†} Nathan J. Patmore,[§] Carly R. Reed,[†] and Claudia Turro^{*,†}

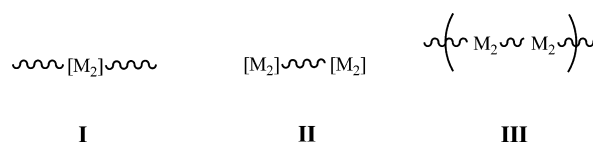
Department of Chemistry, The Ohio State University, 100 West 18th Avenue, Columbus, Ohio 43210-1185, Department of Chemistry, Temple University, 130 Beury Hall, 1901 N. 13th Street, Philadelphia, Pennsylvania 19122, and Department of Chemistry, University of Sheffield, Sheffield S3 7HF, England

Received January 16, 2009

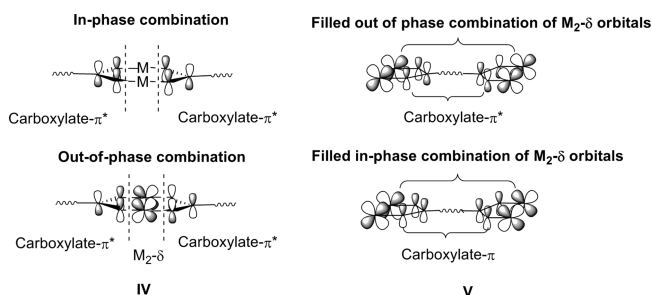
The preparation and characterization (elemental analysis, ^1H NMR, and cyclic voltammetry) of the new compounds $\text{MM}(\text{TiPB})_4$, where $\text{MM} = \text{MoW}$ and W_2 and $\text{TiPB} = 2,4,6\text{-triisopropylbenzoate}$, are reported. Together with $\text{Mo}_2(\text{TiPB})_4$, previously reported by Cotton et al. (*Inorg. Chem.* **2002**, *41*, 1639), the new compounds have been studied by electronic absorption, steady-state emission, and transient absorption spectroscopy (femtosecond and nanosecond). The compounds show strong absorptions in the visible region of the spectrum that are assigned to $\text{MM}\delta$ to arylcarboxylate π^* transitions, $^1\text{MLCT}$. Each compound also shows luminescence from two excited states, assigned as the $^1\text{MLCT}$ and $^3\text{MM}\delta\delta^*$ states. The energy of the emission from the $^1\text{MLCT}$ state follows the energy ordering $\text{MM} = \text{Mo}_2 > \text{MoW} > \text{W}_2$, but the emission from the $^3\text{MM}\delta\delta^*$ state follows the inverse order: $\text{MM} = \text{W}_2 > \text{MoW} > \text{Mo}_2$. Evidence is presented to support the view that the lower energy emission in each case arises from the $^3\text{MM}\delta\delta^*$ state. Lifetimes of the $^1\text{MLCT}$ states in these systems are $\sim 0.4\text{--}6$ ps, whereas phosphorescence is dependent on the MM center: $\text{Mo}_2 \sim 40 \mu\text{s}$, $\text{MoW} \sim 30 \mu\text{s}$, and $\text{W}_2 \sim 1 \mu\text{s}$.

Introduction

We have become interested in the properties of oligothiophenes incorporating MM quadruple bonds.^{1–4} Three classes of compounds exist as depicted by **I–III**, where \sim represents an oligothiophene attached to the dinuclear center. Compounds **I** and **II** may be viewed as models for the extended-chain oligomers/polymers **III**. In order to attach these oligothiophenes to the $[\text{M}_2]$ center, we have employed the use of carboxylates, and a synthetic strategy is outlined in Scheme 1.



The electronic coupling of the MM quadruply bonded unit to the π system of the oligothiophene arises from the interactions of the $\text{M}_2\delta$ and carboxylate π/π^* orbitals as shown in **IV** and **V**.



* To whom correspondence should be addressed. E-mail: chisholm@chemistry.ohio-state.edu (M.H.C.), gustafson@chemistry.ohio-state.edu (T.L.G.), turro@chemistry.ohio-state.edu (C.T.).

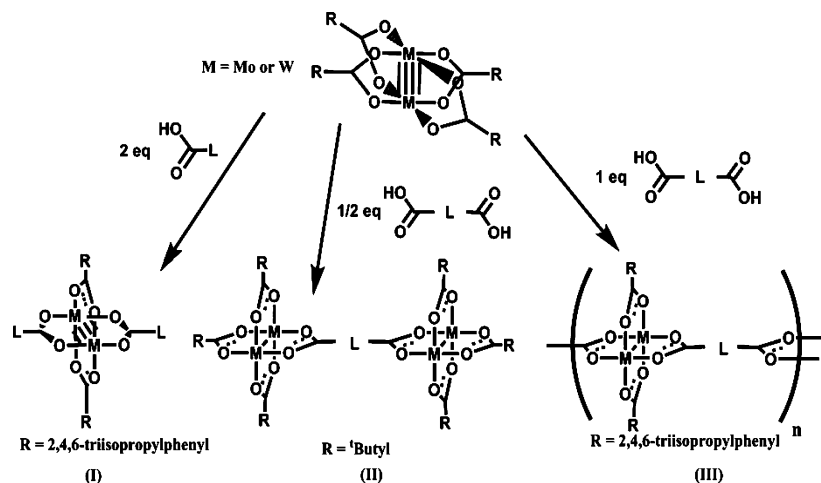
[†] The Ohio State University.

[‡] Temple University.

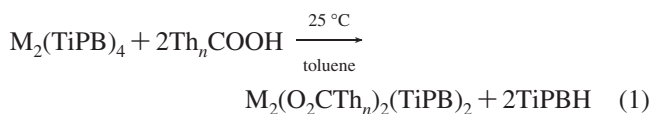
[§] University of Sheffield.

- (1) Burdzinski, G. T.; Chisholm, M. H.; Chou, P. T.; Chou, Y. H.; Feil, F.; Gallucci, J. C.; Ghosh, Y.; Gustafson, T. L.; Ho, M. L.; Liu, Y.; Ramnauth, R.; Turro, C. *Proc. Natl. Acad. Sci. U.S.A.* **2008**, *105*, 15247.
- (2) Byrnes, M. J.; Chisholm, M. H.; Gallucci, J. A.; Liu, Y.; Ramnauth, R.; Turro, C. *J. Am. Chem. Soc.* **2005**, *127*, 17343.
- (3) Chisholm, M. H.; Chou, P.-T.; Chou, Y.-H.; Ghosh, Y.; Gustafson, T. L.; Ho, M.-L. *Inorg. Chem.* **2008**, *47*, 3415.

Scheme 1. General Outline of the Synthesis of Compounds of Type I–III



The electronic coupling of the two thienylcarboxylate ligands as shown in **IV** requires the trans disposition of ligands, and to achieve this, we have employed the ligand substitution reaction shown in eq 1, where TiPB = bulky 2,4,6-triisopropylbenzoate and Th_nCOOH represents an α,α'-linked oligothiophene-2-carboxylic acid.



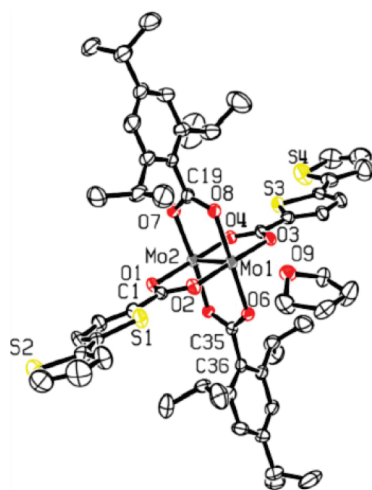
The formation of *trans*-M₂(O₂CTh_n)₂(TiPB)₂ is favored thermodynamically by both steric factors and M₂δ to thienylcarboxylate conjugation, as can be seen from the planar arrangement of thienylcarboxylates in the ORTEP drawing of the bithienylcarboxylate-containing compound shown in Figure 1.¹

The 2,4,6-triisopropylbenzoate of Cr²⁺, Cr₂(TiPB)₄, provided the first structural example of a Cr–Cr quadruple bond without axial coordination to the Cr₂⁴⁺ center.⁵ The short Cr–Cr distance of 1.9662 Å validated Cotton's hypothesis that the Cr–Cr quadruple bond distance was inversely related

to the strength of the axial ligation. Subsequently, Cotton and co-workers reported the preparation of the Mo₂⁴⁺-containing analogue, Mo₂(TiPB)₄.⁶ Our interest in the polymers of type **III** and the model compounds, **I**, led us to prepare the related complexes MoW(TiPB)₄ and W₂(TiPB)₄, which we report herein, together with their electrochemical and spectroscopic characterization. Of particular interest are the photophysical properties of the series MM(TiPB)₄, where MM = Mo₂, MoW, and W₂. Rather surprisingly, given the extensive chemistry of these dinuclear carboxylates,⁷ the photophysical properties have received little attention for nearly 30 years following the work of Trogler et al. on Mo₂(O₂CCF₃)₄.⁸ A knowledge and understanding of the photophysical properties of these compounds is clearly pertinent to studies of their derivatives formed in eq 1. In particular, it is important to be able to distinguish between ¹MLCT and ³MMδδ* emissive states.

Results and Discussion

The preparation of the new compounds MoW(TiPB)₄ and W₂(TiPB)₄ involved modified procedures for the related dinuclear pivalates.^{9,10} Details are described in the Experimental Section. The new compounds are air-sensitive and readily oxidized. Thus, their preparation and handling require the use of rigorously dried and oxygen-free solvents and atmospheres. The compounds are orange (MoW) and red



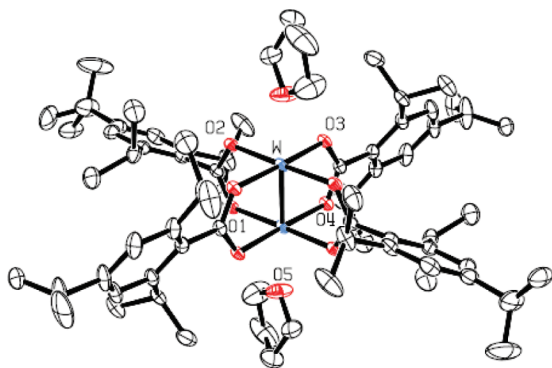


Figure 2. ORTEP drawing of the molecular structure of $W_2(TiPB)_4 \cdot 2THF$ showing the atom numbering scheme. The ORTEP plot is drawn with 30% probability displacement ellipsoids for the non-H atoms. All of the H atoms are omitted for clarity.

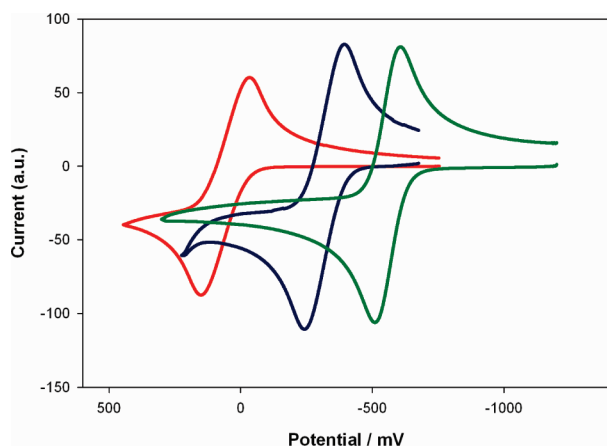


Figure 3. Cyclic voltammetry representing oxidation of the MM center in $MM(TiPB)_4$ complexes, where red = Mo_2 , blue = MoW , and green = W_2 . Oxidation potentials are referenced with respect to the $Cp_2Fe^{0/+1}$ couple.

(W_2) and hydrocarbon-soluble; they give molecular ions $MM(TiPB)_4^+$ in the mass spectrum by matrix-assisted laser desorption/ionization time-of-flight (MALDI-TOF) mass spectroscopy.

Solid-State and Molecular Structures of $W_2(TiPB)_4 \cdot 2THF$. An ORTEP drawing of the $W_2(TiPB)_4 \cdot 2THF$ molecule is given in Figure 2. In the space group $P\bar{1}$, there are two unique benzoate ligands and one unique W atom. The W–W distance of 2.1935(2) Å is typical of a W–W quadruple bond. The four unique W–O carboxylate distances are in the range of 2.07–2.09 Å. The THF molecule is only weakly ligated, as evidenced by the long $W \cdots O$ distance of 2.574 Å. Pertinent to the electronic structure of the molecule is the arrangement of the planes of the arylcarboxylates. The dihedral angles between the respective O_2C and C_6 planes are 29° and 67°. As can be seen from Figure 1 and from an inspection of the molecular structures of $W_2(TiPB)_2(O_2C-6\text{-azulenecarboxylate})_2$ ¹¹ and $W_2(TiPB)_2(nic)_2$, where nic = 4-isonicotinate,¹² the TiPB ligands are arranged such that their C_6 and O_2C planes are close to 90°. This minimizes $M_2\delta$ to arene π^* interactions and allows maximum trans $L-M_2-L$ conjugation. In the $M_2(TiPB)_4$ structures, this arrangement is not possible for steric reasons, but with a dihedral angle of 29°, two of the

Table 1. Spectroscopic, Electrochemical, and Kinetics Data for $MM(TiPB)_4$ Compounds

complex	λ_{abs} (nm)	λ_{em} (nm)	E_{ox} (V)	τ_{MLCT} (ps)	$\tau_{\delta\delta^*}$ (μ s)
$Mo_2(TiPB)_4$	388	445, 1100	+0.08	6.0 ± 0.5	43 ± 0.4
$MoW(TiPB)_4$	430	504, 980	−0.32	0.45 ± 0.02	27 ± 0.2
$W_2(TiPB)_4$	480	555, 815	−0.55	0.37 ± 0.02	1.6 ± 0.03

trans-aryl groups enjoy significant $M_2\delta$ to ligand π^* back-bonding.

Electrochemical Studies. The compounds show reversible oxidation waves in their cyclic voltammograms assignable to the removal of an electron from the $M_2\delta$ orbital, as shown in Figure 3, and their half-wave potentials are listed in Table 1. The ease of oxidation increases with the W content in the central MM unit, which is consistent with the known chemistry of related MM multiply bonded complexes (Table 1).¹³

Electronic Absorption Spectra. The absorption spectra for the three $MM(TiPB)_4$ compounds are shown in Figure 4. The strong absorption bands in the visible region arise from MLCT transitions, $MM\delta$ to arylcarboxylate π^* . Consistent with expectations based upon the oxidation potentials, inspection of Table 1 reveals that the absorption maxima are red-shifted with increasing W content in the MM bond. The weaker $MM \delta$ to δ^* transition, which is expected⁷ around $\lambda_{max} \sim 450$ nm, is clearly masked in each case by the intense MLCT absorption.

Steady-State Emission Spectra. Excitation into the MLCT peak of each complex in a THF solution leads to weak emission in the visible region of the spectrum and stronger emission in the near-IR region (Figure S1 in Supporting Information and Figure 5, respectively). The relative energy of the higher energy emission follows the same energy trend as that of the ¹MLCT absorption: $MM = Mo_2 > MoW > W_2$. This higher energy emission is assigned as arising from a MLCT state, owing to the small Stokes shift from the ¹MLCT absorption. In contrast, the energy of the near-IR luminescence is in the inverse order of the ¹MLCT absorption, namely, $MM = W_2 > MoW > Mo_2$ (Table 1). The emissions from the $Mo_2(TiPB)_4$, $MoW(TiPB)_4$, and $W_2(TiPB)_4$ compounds show clear evidence of vibronic features that correlate with $\nu(MM) \sim$

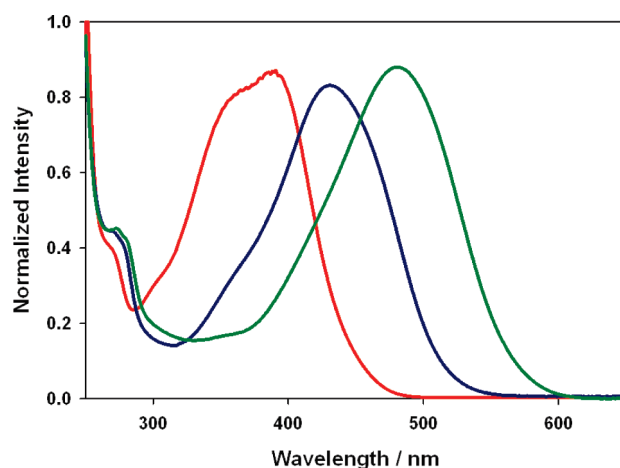


Figure 4. Absorption spectra of $MM(TiPB)_4$ complexes, where red = Mo_2 , blue = MoW , and green = W_2 .

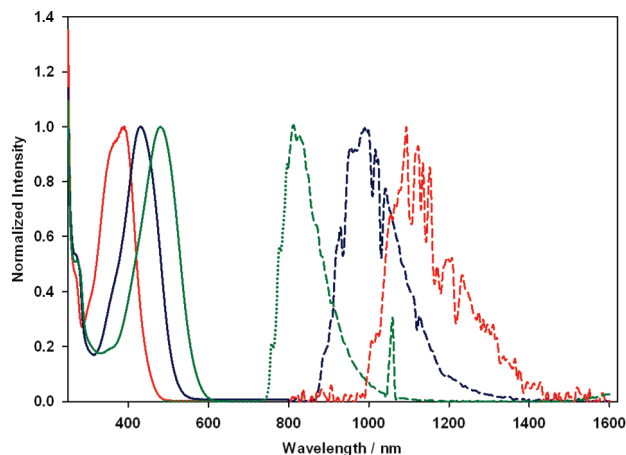


Figure 5. Absorption spectra (solid lines) in THF at room temperature and near-IR emission spectra (dashed lines) in 2-MeTHF at 77 K for $\text{MM}(\text{TiPB})_4$ complexes, with $\lambda_{\text{ex}} = 405$ nm for $\text{MM} = \text{Mo}_2$ and MoW and $\lambda_{\text{ex}} = 532$ nm for $\text{MM} = \text{W}_2$, where red = Mo_2 , blue = MoW , and green = W_2 solution.

$350\text{--}400\text{ cm}^{-1}$. We also note that the maximum of the low-energy emission of $\text{Mo}_2(\text{TiPB})_4$ is nearly identical with that of the $\text{Mo}_2(\text{TiPB})_2(\text{O}_2\text{CTh}_n)_2$ ($n = 1\text{--}3$) compounds, albeit weaker and less structured.¹ These data taken together lead us to assign the near-IR emission as arising from the $^3\text{MM}\delta\delta^*$ state of each complex.

Transient Absorption Spectra. The three compounds $\text{MM}(\text{TiPB})_4$ were examined by femtosecond and nanosecond transient absorption spectroscopy in THF. With excitation at 365 nm, where $\text{MM} = \text{Mo}_2$ and MoW , and excitation at 514 nm, where $\text{MM} = \text{W}_2$, the $\text{MM}(\text{TiPB})_4$ compounds showed the presence of intermediate short-lived states, with lifetimes of ~ 6 ps, ~ 500 fs, and ~ 390 fs, respectively. The trends of the lifetimes of the Mo_2 -, MoW -, and W_2 -containing compounds are consistent with the expected increased rate of intersystem crossing (ISC) as a function of the increased spin–orbit coupling (heavy-atom effect) across the series. Therefore, this intermediate short-lived state and its corresponding high-energy emission have been assigned as arising from the $^1\text{MLCT}$ state in each compound, which undergoes ISC to generate the long-lived $^3\text{MM}\delta\delta^*$ state. The lifetimes of the $^3\text{MM}\delta\delta^*$ states of the $\text{MM}(\text{TiPB})_4$ complexes are also dependent on the metal, with $\tau \sim 40\text{ }\mu\text{s}$ for $\text{MM} = \text{Mo}_2$, $\tau \sim 30\text{ }\mu\text{s}$ for $\text{MM} = \text{MoW}$, and $\tau \sim 2\text{ }\mu\text{s}$ for $\text{MM} = \text{W}_2$. For each complex, the lifetime of this long-lived state was determined from the ground-state bleaching observed in its transient absorption spectrum ($\lambda_{\text{exc}} = 355$ nm; fwhm ~ 8 ns). Similar to the trend for the observed rate of ISC from $^1\text{MLCT} \rightarrow ^3\text{MM}\delta\delta^*$ described above, the lifetime of the decay from the emissive $^3\text{MM}\delta\delta^*$ state to the $^1\text{MM}\delta^2$ ground state is also dependent on the content of the heavy metal. It is evident from Table 1 that the lifetimes of the $^3\text{MM}\delta\delta^*$ states, $\tau_{\delta\delta^*}$, follow the order $\text{Mo}_2 > \text{MoW} > \text{W}_2$. It should be noted that the lifetimes of the $\text{MM}(\text{TiPB})_4$ complexes are comparable to those recently reported by us for $\text{M}_2(\text{O}_2\text{CAR})_4$ compounds ($\text{M} = \text{Mo}$ or W ; $\text{Ar} = \text{phenyl}$, naphyl , and 9-anthracenyl), which also possessed both short-lived $\tau \sim 10$ ps and long-lived $\tau \sim 50\text{--}60\text{ }\mu\text{s}$ excited states.² In this earlier study, we proposed that the long-lived state was

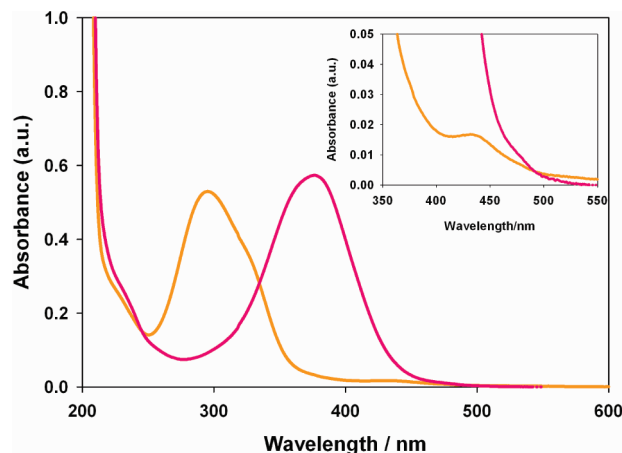


Figure 6. Absorption spectra of $\text{M}_2(\text{O}_2\text{CtBu})_4$ compounds, where $\text{M} = \text{Mo}$ (orange) and $\text{M} = \text{W}$ (pink).

$^3\text{MLCT}$. Given the present study, we now believe that the long-lived state should be assigned as $^3\text{MM}\delta\delta^*$.

Emissive Studies on Related Dinuclear Compounds. The dimetal tetraalkanoates of dimolybdenum and ditungsten do not have intense absorptions in the visible region of the spectrum because the $\text{M}_2\delta$ to $\text{CO}_2\pi^*$ transition occurs at higher energy. These compounds are yellow-orange as a result of the tailing of this absorption into the visible region of the spectrum. The absorption spectra of the pivalates are compared in Figure 6. In each case, the appearance of $^1\text{MM}\delta\delta^*$ is much weaker and appears at ~ 450 nm for dimolybdenum tetrapivalate, while it is completely masked by a stronger $^1\text{MLCT}$ absorption for ditungsten tetrapivalate. With excitation at 405 nm, the latter shows an emission in near-IR, which is very similar in shape and energy to that observed for $\text{W}_2(\text{TiPB})_4$. This leads us to conclude that the near-IR emission observed for $\text{W}_2(\text{Piv})_4$ also arises from $^3\text{WW}\delta\delta^*$. Related dinuclear complexes such as $\text{K}_4\text{Mo}_2\text{Cl}_8$ ¹⁴ and $\text{Mo}_2\text{Cl}_4(\text{PR}_3)_4$ ^{15,16} have been shown to exhibit $^1\text{MM}\delta\delta^*$ emission in the visible region, but to our knowledge, no near-IR emission from $^3\text{MM}\delta\delta^*$ has been previously reported and in this regard the $\text{MM}(\text{TiPB})_4$ compounds are unique. We note that, in the original spectroscopic study of $\text{Mo}_2(\text{O}_2\text{CCF}_3)_4$, a weak but structured emission at 1.3 K was reported and assigned to a $^3\text{MM}\delta\pi^*$ state.⁸ This is now reasonably assigned as $^1\text{MM}\delta\delta^*$, given our current understanding of the electronic structure of these quadrupty bonded compounds.

Concluding Remarks

The preparations of the new compounds $\text{MoW}(\text{TiPB})_4$ and $\text{W}_2(\text{TiPB})_4$ allow for the synthesis of a complete series of compounds and oligomers of the type depicted in **I–III**. The variation in MM affords a unique opportunity to study the influence of each metal on the ground and photoexcited states. The series of compounds $\text{MM}(\text{TiPB})_4$ ($\text{MM} = \text{Mo}_2$,

(14) Trogler, W. C.; Solomon, E. I.; Gray, H. B. *Inorg. Chem.* **1977**, *16*, 3031.

(15) Hopkins, M. D.; Gray, H. B. *J. Am. Chem. Soc.* **1984**, *106*, 2468.

(16) Miskowski, V. M.; Goldbeck, R. A.; Kliger, D. S.; Gray, H. B. *Inorg. Chem.* **1979**, *18*, 86.

MoW, and W₂) are themselves interesting in showing both fluorescence and phosphorescence. It is also noteworthy that the energy of the ³MMδδ* state, which follows the order MM = W₂ > MoW > Mo₂, is in the inverse order of the ¹MLCT energies and, furthermore, that the related *n*-alkylanoates M₂(O₂CBu¹)₄ have only very weakly emitting triplet states. These data will aid in the interpretation of the emissive properties of the model compounds of type **I** and **II** and the oligomers of type **III**.

Experimental Section

Measurements. NMR spectra were recorded on a 400 MHz Bruker DPX Advance 400 spectrometer. All ¹H NMR chemical shifts are in ppm relative to the protio impurity in benzene-*d*₆ at 7.12 ppm.

Electronic spectra at room temperature were recorded using a Perkin-Elmer Lambda 900 spectrometer in a THF solution. A 10.00 mm IR quartz cell was employed.

The cyclic and differential pulse voltammograms of all of the complexes were collected at a scan rate of 100 and 5 mV s⁻¹, respectively, using a Princeton Applied Research (PAR) 173A potentiostat–galvanostat equipped with a PAR 176 current-to-voltage converter. Electrochemical measurements were performed under an inert atmosphere in a 0.5 M solution of ¹⁸Bu₄NPF₆ in THF inside a single-compartment voltammetric cell equipped with a platinum working electrode, a platinum wire auxiliary electrode, and a pseudo reference electrode consisting of a silver wire in 0.5 M ¹⁸Bu₄NPF₆/THF separated from the bulk solution by a Vycor tip. The potential values are referenced to the FeCp₂/FeCp₂⁺ couple, obtained by the addition of a small amount of FeCp₂ to the solution.

Nanosecond transient absorption measurements were carried out in 1 × 1 cm² quartz cuvettes equipped with Kontes stopcocks. Nanosecond transient absorption spectra were measured on a home-built instrument pumped by a frequency-doubled (532 nm) or -tripled (355 nm) Spectra-Physics GCR-150 Nd:YAG laser (fwhm ~ 8 ns, ~ 5 mJ per pulse). The signal from the photomultiplier tube (Hamamatsu R928) was processed by a Tektronics 400 MHz oscilloscope (TDS 380) (Byrnes, M. J.; Chisholm, M. H.; Gallucci, J. A.; Liu, Y.; Ramnauth, R.; Turro, C. J. *Am. Chem. Soc.* **2005**, *127*, 17343–17352).

The steady-state near-IR luminescence measurements at 77 K were carried out in J. Young NMR tubes. The spectra were measured on a home-built instrument utilizing a germanium detector. The sample was excited at 658 nm (laser diode max power: 65 mW), and a RG830 long-pass filter was placed between the sample and detector.

In the femtosecond transient absorption experiments, samples were excited at 365 nm for Mo₂ and MoW and at 514 nm for W₂ (with excitation power ~ 1–2 μJ at the sample). Using standard glovebox techniques, samples were prepared having an absorbance ~ 0.4–0.8 at the excitation wavelength and contained in a 10.0 × 1.0 mm² quartz cuvette (Starna Cells, Inc.) that was modified with a Kontes stopcock. The laser and detection systems that were used have been described in detail previously (Burdzinski, G.; Hackett, J. C.; Wang, J.; Gustafson, T. L.; Hadad, C. M.; Platz, M. S. *J. Am. Chem. Soc.* **2006**, *128*, 13402). During the measurements, the samples were kept in constant motion by manual movement of an XYZ stage in the vertical and horizontal directions. To ensure that no photodecomposition occurred during data collection, absorption spectra were recorded before and after the transient absorption measurements. The measurements were repeated five times at each

of the pump–probe delay positions to confirm data reproducibility throughout the experiment, and the resulting spectra were corrected for the chirp in the white-light supercontinuum.¹¹ The kinetics were fit to a single-exponential decay of the form $S(t) = A \exp(-t/\tau) + C$, with amplitude *A*, lifetime *τ*, and offset *C*, using *SigmaPlot 10.0*. Error bars for the lifetimes are reported as standard errors of the exponential fit.

Microanalysis was performed by Atlantic Microlab Inc.

MALDI-TOF mass spectrometry was performed on a Bruker Reflex III (Bruker, Bremen, Germany) mass spectrometer operated in a linear, positive-ion mode with an N₂ laser. Dithranol was used as the matrix and prepared as a saturated solution in THF. Allotments of matrix and sample were thoroughly mixed together; 0.5 mL of this was spotted on the target plate and allowed to dry.

Synthesis. All reactions were carried out under 1 atm of oxygen-free UHP-grade argon using standard Schlenck techniques or under a dry and oxygen-free nitrogen atmosphere using standard glovebox techniques. All solvents were dried and degassed by standard methods and distilled prior to use.

MoW(TiPB)₄. Mo(CO)₆ (1.58 g, 5.98 mmol), W(CO)₆ (6.33 g, 17.9 mmol), and 2,4,6-triisopropylbenzoic acid (TiPB-H; 12 g, 48.3 mmol) were dissolved in 90 mL of dry 1,2-dichlorobenzene and 15 mL of dry THF and allowed to reflux at 150 °C for 3 days under an argon atmosphere. After 3 days, the mixture had turned dark brown. The solvents were removed, and the product was suspended in hexanes and isolated as an orange solid. NMR indicated an approximate Mo₂(TiPB)₄ to MoW(TiPB)₄ ratio of 30% to 70%. After calculation of the requisite amount of oxidizing agent required to oxidize MoW(TiPB)₄, approximately 5.42 g of the mixture was dissolved in benzene and 0.39 g of I₂ dissolved in benzene was added. This was allowed to stir at room temperature for 2 h, and the solvent was removed in vacuo. Diethyl ether was added to this, and a pale-green solid was isolated by filtration. The solid was then stirred overnight with zinc dust (5 g) in acetonitrile. The solvent was removed, then diethyl ether was added, and the whole suspension was filtered through Celite. The filtrate was dried to afford 2.25 g of an orange solid. Recrystallization from THF gave large orange crystals.

Microanal. Calcd for C₆₄H₉₂MoO₈W: C, 60.56; H, 7.31. Found: C, 60.51; H, 7.24. NMR (benzene-*d*₆, 400 MHz): δ_H 7.25 (s, 8H), 3.67 (m, 8H), 2.80 (m, 4H), 1.33 (d, 48H, *J*_{HH} = 7 Hz), 1.22 (d, 24H, *J*_{HH} = 7 Hz). MALDI-TOF. Calcd monoisotopic MW for C₆₄H₉₂MoO₈W: 1269.19. Found: 1269.9 (M⁺).

W₂(TiPB)₄. WCl₄ (7.81 g, 23.9 mmol) was weighed out in a 250 mL Schlenk flask and suspended in ~60 mL of ice-cold dry THF, and the flask was placed in an ice bath. In the glovebox, a 500 mL Schlenck flask was used to make Na/Hg using 1.38 g of Na and 17.09 mL of Hg. To the amalgam was carefully added 15.5 g of a sodium salt of 2,4,6-triisopropylbenzoic acid (TiPB-Na). After this, the flask was put on the Schlenk line and cooled over an ice bath. To it was added the suspension of WCl₄ and some more ice-cold THF, and the mixture was allowed to stir for 30 min at 0 °C. Later, this was brought up to room temperature and allowed to stir overnight. The mixture was then filtered over Celite, and the filtrate was collected and reduced in volume. This was then cooled in the refrigerator overnight to give red crystals and filtered and recrystallized from THF to give 14 g (86%) of a red solid.

Microanal. Calcd for C₆₄H₉₂O₈W₂: C, 56.64; H, 6.83. Found: C, 56.69; H, 6.89. NMR (THF-*d*₈, 400 MHz): δ_H 7.16 (s, 8H), 3.45 (m, 8H), 2.95 (m, 4H), 1.29 (d, 12H, *J*_{HH} = 7 Hz), 1.20 (d, 24H,

$J_{\text{HH}} = 7$ Hz). MALDI-TOF. Calcd monoisotopic MW for $\text{C}_{58}\text{H}_{60}\text{O}_8\text{S}_6\text{W}_2$: 1357.09. Found: 1358 (M^+).

Acknowledgment. We thank the National Science Foundation for support of this work along with the Ohio State Institute for Materials Research and the Ohio State Photovoltaic Innovation Center.

Supporting Information Available: Listing of crystallographic data in CIF format for the compound $\text{W}_2(\text{TiPB})_4$ and singlet emission spectra for the compounds $\text{MM}(\text{TiPB})_4$ where $\text{MM} = \text{Mo}_2$, MoW , and W_2 . This material is available free of charge via the Internet at <http://pubs.acs.org>.

IC900092C